Biochimica et Biophysica Acta 900 (1987) 45–55
Elsevier

BBA 73573

The effect of mercuric salts on the electro-rotation of yeast cells and comparison with a theoretical model

Birgitta M. Geier, Barbara Wendt, W. Michael Arnold and Ulrich Zimmermann

Lehrstuhl für Biotechnologie der Universität Würzburg, Röntgenring 11, Würzburg (F.R.G.)

(Received 29 December 1986)
(Revised manuscript received 10 March 1987)

Key words: Cell rotation; Toxin; Mercuric salt; Electro-rotation; Cell-wall conductivity; (*S. cerevisiae*)

The rotational spectrum of yeast cells changed after pre-treatment of the cells with $HgCl_2$ or $Hg(NO_3)_2$ and became indistinguishable from that of ultrasonically produced cell walls. The spectrum of the affected cells contained a peak which could only be explained by attributing a conductivity to the cell walls that was higher than that of the medium. Theoretical models of the rotational response are fully in accord with the experimental spectra. It is shown that the rotation method is capable of measuring even the low cell wall conductivity of yeast cells (which was found to be 33 μS/cm at 10 μS/cm medium conductivity). Knowledge of the spectra allowed a field frequency to be selected at which untreated cells showed no rotation, but at which cells affected by treatment with Hg(II) identified themselves by rotating in the same direction as the field. Calculation of the percentage of cells showing this co-field rotation gave an index (termed the co-field rotation value) of the proportion of the cells that were affected. Using this technique, effects of 25 nmol/l Hg(II) could be demonstrated. In media of low conductivity (10 μS/cm) the change in the rotational spectrum was usually 'all-or-none', whereas at 200 μS/cm a graded Hg(II)-mediated change became apparent. The co-field rotation method showed that the action of small quantities of Hg(II) was still increasing after 3 h of incubation and paralleled the Hg(II)-induced K^+ release. A rapid reduction of the effects of Hg(II) was seen when 3–30 mM K^+ (or Na^+) or when 1 mM Ca^{2+} were present in the incubation medium, or as the pH was increased. At high incubation cell concentrations the toxic effect of Hg(II) was reduced, apparently due to binding by the cells.

Introduction

The observation of the effects of ecotoxins such as mercuric compounds on living cells is not only of interest in its own right, but also for the development of bio-assays. Hg(II) compounds are known to permeabilise the plasmalemma of yeast [1,2] and of other cells [3–5]. Hg-permeabilised yeast cells lose much of their K^+ and anion content [6]. When comparing toxicity data obtained with Hg compounds, it must be remembered that the Hg^{2+} ion has a strong tendency to form complex species [7], and that some of these complexes are membrane permeable [8–10]. Which complex is dominant in any particular medium will depend strongly on the concentrations of ligands present.

The above observations on the membrane per-

Abbreviations: Hg(II), bivalent mercury, whether present as Hg^{2+}, molecular $HgCl_2$ or a complex ion; Mes, 4-morpholine-ethanesulphonic acid.

Correspondence: B.M. Geier, Lehrstuhl für Biotechnologie der Universität Würzburg, Röntgenring 11, D-8700 Würzburg, F.R.G.

meability increase caused by Hg(II) compounds indicate that the method of rotation of single cells in a rotating electrical field may be useful for the quantification of this effect. The theory and practice of cell rotation are now reasonably well established [11–17].

In the following section we present results of models based on likely yeast cell properties, for both control and permeabilised cells. The insight gained from these model calculations is then used to interpret the change in the rotation spectrum caused by treatment with Hg(II). We go on to show how the sensitivity of this technique can be modulated by a variety of incubation conditions.

It should be noted that the permeabilisation of yeast cells by various chemicals has been observed before using electrical measurements [2,18]. However, those measurements applied dielectric bridge techniques to yeast suspensions, and were therefore not able to observe the all-or-none response seen here with the single-cell technique.

We have already described [19] how Ag^+ rapidly affects the rotation of yeast cells. Hg(II) can be expected to act differently, because of the above-described tendency to form complex species. The results show that Hg(II) differs from Ag^+ not only in the chemical conditions that favour its action, but also in the speed and extent of the membrane damage that are caused.

Materials and Methods

A rotating field of 120 V/cm field strength was generated within a four-electrode chamber [13,16,20]. Apart from the spectra given in Figs. 3 and 4, all measurements used a fixed frequency of 300 kHz. The cells were observed as described by Arnold et al. [19].

Use of a 300 kHz rotating field in 10 μS/cm media gave no rotation in most control cells, but did give a co-field rotation in Hg(II)-pretreated cells (see legend to Fig. 3). When assessing a large number of cells it was found convenient to express the degree of change as the co-field rotation (CFR):

$$\mathrm{CFR} = \frac{\{(\text{No. cells co-field}) - (\text{No. cells anti-field})\} \times 100}{\text{Total number of cells (co-field + stationary + anti-field)}} \quad (1)$$

Solutions of Hg(II) salts were prepared fresh daily. In the case of the acetate or nitrate, the first solution was diluted within 15 min, to avoid the formation of a red precipitate (presumably of $Hg(OH)_2$). The incubations and the final dilutions of mercuric compounds were carried out in plastic test tubes (to preclude adsorbtion on glassware).

We show later that the concentration of free Hg(II) added to cell suspensions is considerably reduced by binding to the cells. Therefore, we have distinguished between the total amount of Hg(II) present per unit volume suspension (expressed in, e.g., μmol/l) and the concentration of unbound Hg(II) (expressed in, e.g., μM).

The same strain of bottom-fermenting brewers' yeast was used and grown as before [19]. A synthetic medium was used for consistency and to minimise carry-over of those nutrients which may complex heavy metals [21–23].

Hg-treatment used the same procedure as described by Arnold et al. [19]. If not otherwise stated the cells were incubated at 30 °C for 3 h: incubations at 20 °C gave a much lower sensitivity to Hg(II). After washing, the cells were re-suspended and brought to the rotation-assay conductivity (10.0 ± 0.1 μS/cm) by addition of 2.5 mM KCl solution.

For investigation of the K^+ loss induced by mercury (II), no buffer was used in the incubations (although the pH was adjusted to 4.5 by addition of citric acid).

Yeast cell rotation modelled

The response induced by a rotating electrical field in spherical cells has been thoroughly analyzed by Sauer and Schlögl [15] and, using a different approach, by Fuhr [16,17]. For a simple model cell (a conductive spherical droplet bound by a single thin membrane without surface charge or conductivity), and assuming the medium behaves as a simple dielectric, the two treatments produce identical results. Sauer and Schlögl also predict an additional rotation peak due to the effects of the relaxation generated by counter ions loosely bound to a true surface charge. However, this additional peak does not appear in the rotation spectra that we have taken (very possibly the frequency range must be extended downwards). On the other hand, Fuhr has explicitly considered

the effects of a surface conductance and we shall show that the results agree very well with this theory. The rotational torque equation used as the basis of the model is Eqn. 123 (combined with the hydrodynamic Eqn. 84) of Ref. 16, to which the interested reader is referred. We point out that the usual area-specific quantities membrane conductivity (G_m, units S/m^2) and membrane capacity (C_m, units F/m^2) are used here. However, Eqn. 123 of Ref. 16 uses properties of bulk materials: these are the membrane-material conductivity (σ_2, units S/m) and absolute permittivity (ϵ_2, units F/m). These two sets of parameters are inter-related by the membrane thickness, d, as follows (if $d \ll$ cell radius):

$G_m = \sigma_2/d$, and $C_m = \epsilon_2/d$.

The legends to Figs. 1 and 2 give the parameters we used in the model. It can be seen that a

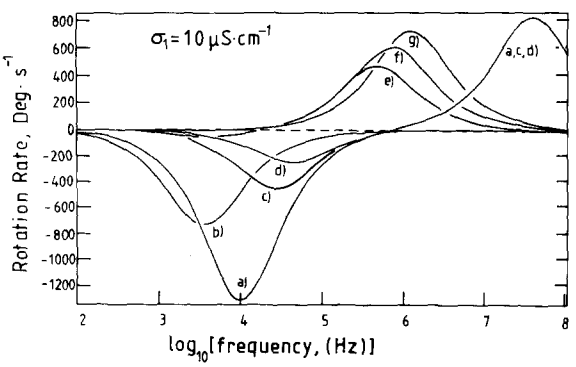

Fig. 1. Theoretical rotation spectra for spherical model cells in a medium of conductivity 10 μS/cm and viscosity 10 mP at a field strength of 96 V/cm (parallel conditions to those of Fig. 3). Curves a, c and d refer to model cells in which the internal conductivity is high (5 mS/cm), the membrane conductivity is low (0.33 mS/cm^2) but with increasing surface conductances of: a, $K_s = 0$; c, $K_s = 5$ nS; d, $K_s = 10$ nS. As described in the text, these surface conductances are equivalent to additional membrane conductivities of 0, 0.11 and 0.22 S/cm^2, respectively. Curves b, e, f and g refer to models in which the inner conductivity is equal to that of the medium, the membrane conductivity is low (0.33 mS/cm^2), but with surface conductances of: b, $K_s = 0$; e, $K_s = 5$ nS; f, $K_s = 10$ nS; g, $K_s = 20$ nS. In such a model the effects of surface conductance and membrane conductivity are not equivalent. Other parameters were taken to be: membrane thickness, 3 nm; cell radius, 3 μm; outside and inside permittivities 80·88.54 fF/cm, membrane permittivity, 3.3·88.54 fF/cm (giving $C_m = 0.97$ μF/cm^2).

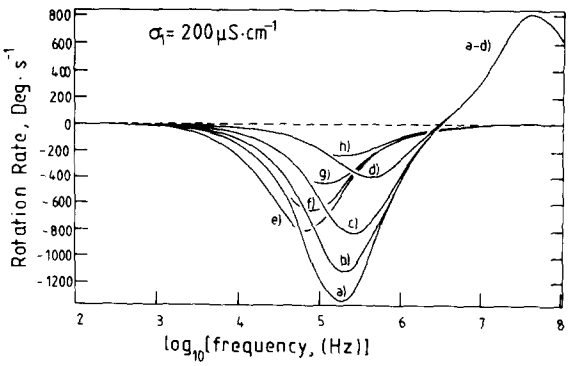

Fig. 2. Theoretical rotation spectra for spherical model cells in a medium of conductivity 200 μS/cm and viscosity 10 mP at a field strength of 96 V/cm (parallel conditions to those of Fig. 4). Curves a–d refer to models with a high inner conductivity (5 mS/cm) and a low membrane conductivity (0.33 mS/cm^2), but with increasing surface conductances, as follows: a, $K_s = 0$ nS; b, $K_s = 10$ nS; c, $K_s = 30$ nS; d, $K_s = 100$ nS. Curves e–h refer to cell models in which the inner conductivity is equal to that of the medium, and the surface conductance is zero. The membrane conductivity was increased as follows: e, $G_m = 0.33$ mS/cm^2; f, $G_m = 0.1$ S/cm^2; g, $G_m = 0.33$ S/cm^2; h, $G_m = 1.0$ S/cm^2. The 'other parameters' are as given for Fig. 1.

protoplast (a normal cell less its wall) in medium of conductivity (σ_1) of 10 μS/cm should behave as in curve a of Fig. 1 (1a). In a model with no surface conductance, the frequency of the anti-field maximum is determined essentially by the membrane conductivity and capacity, together with the conductivity of the medium (as long as this remains much lower than that of the cell interior). For example, increasing σ_1 by a factor of 20 (curve a, Fig. 2 (2a) increases the anti-field peak frequency by the same factor. This does agree substantially with the simple equations presented earlier [11,13] and it is to this peak that the majority of the work so far published refers.

The high frequency peak (which is co-field in all cases of biological interest) is predicted to be essentially independent of the membrane. This can be expected if the membrane is considered to be electrically transparent at high frequencies. This rotation at high frequencies depends on the difference in dielectric properties between the cell interior and the medium. If the high conductivity typical of the interior of a healthy cell is decreased to that of the medium, then the high frequency peak disappears, see curve b of Fig. 1 (1b) and

curve e of Fig. 2 (2e). However, the low-frequency anti-field peak is only somewhat reduced in amplitude (but is still present). Only when the membrane resistivity is much reduced (curves c and d of Fig. 1 (1c, 1d) also f–h of Fig. 2 (2f–h) does the anti-field rotation also become much weaker. The biological interpretation is that curve 1a corresponds to an undamaged cell, curve 1b to a cell without membrane damage but with total loss of ionic contents, and curves 1c and 1d to cells in which the membrane is relatively conductive.

However, examination of the effects of surface conductance (K_s) on rotation spectra show that it produces exactly the same change in curve 1a as increasing the membrane conductivity does, at least in the case of cells with high internal conductivity. For such cells we can use [14]:

$$a^2 G_m = 2K_s \tag{2}$$

to relate the values of these two distinct parameters which produce the same effect. That means that curves 1c and 1d correspond either to membrane conductivities of 0.11 S/cm^2 and 0.22 S/cm^2, respectively, or to K_s values of 5 nS and 10 nS, respectively (or to some combination).

On the other hand, modelling of the effects of G_m and of K_s show that these quantities have very different effects in the case where the inner conductivity is equal to that of the medium. Increasing the G_m value causes the peak of curve 1b to reduce in amplitude, eventually to zero. On the other hand, curve 1e shows how increasing K_s to 5 nS causes a new positive peak to appear. This peak increases in amplitude and frequency as K_s is increased, as shown by curves 1f ($K_s = 10$ nS) and 1g ($K_s = 20$ nS). It is significant that increasing the membrane conductivity has no influence on these curves, as long as the inside conductivity does not exceed that of the medium.

At 200 μS/cm medium conductivity, the effects of a given amount of K_s (or G_m), are qualitatively the same as at 10 μS/cm, but much weaker. The curve series 2a–d (K_s values of 0, 10, 30 and 100 nS) shows that (compare with curves 1a, 1c and 1d) the reduction in the effect of K_s on a cell of high internal conductivity is in proportion to the increase in σ_1 (a factor of 20). The curve series 2e–h (G_m values of 0, 0.1, 0.3 and 1 S/cm^2) shows the effect of increasing membrane conductance (maintaining $K_s = 0$) on 'cells' with equalised internal and external conductivities. This data is discussed further below.

The above has relied heavily upon the concept of surface conductance without mentioning a physical basis for this. It is now necessary to show that the cell wall can provide this conductivity, although the typical thickness of this organelle of about 0.3 μm [24,25] means that quantitative conclusions based on 'surface' conductivity must be considered approximate.

There is good evidence that, due to the counter-ions to the fixed charges present in the cell wall, the conductivity can be many times that of the medium. This has been measured in certain bacteria [26,27] and the conductivity ratio was greatest at low medium conductivities. In addition, it has been suggested that the cell walls of micro-organisms can contribute to a distinct type of co-field cell rotation [20]. There appear to be no direct measurements of the electrical properties of yeast cell wall material. However, it is known that yeast walls are highly porous [28,29]. As argued at the end of this section they can, therefore, be assumed to have a dielectric constant close to that of the medium. It has been suggested from electrophoretic measurements that the yeast cell wall (like bacterial walls) is conductive [30], however, no quantitative estimate of this conductivity in the case of yeast is available. The bacterial data obtained using dielectric measurements on whole cells [26] suggest conductivies of the wall material (in low-conductive media, such as used here) of 3 mS/cm for *Escherichia coli* and of 9 mS/cm for *Micrococcus lysodeikticus*. Work on isolated walls from *M. lysodeikticus* [27] gave a value of 4 mS/cm, although this was possibly lowered by the isolation procedure.

The conductance, along the plane of the layer, of a wall of conductivity σ_w and thickness, w, is given by:

$$K_w = \sigma_w \cdot w \tag{3}$$

In order to have the same total conductance, the conductance that must be assigned to a true surface layer without thickness is given by:

$$K_s = (\sigma_w - \sigma_1) w \tag{4}$$

where the conductance of the medium that occupies the volume formerly occupied by the wall is taken into account. If the cell wall is assumed to be homogeneous and of thickness 0.3 μm, then the values of σ_w given above would result in surface conductivity values between 90 and 270 ns. As shown in Figs. 1 and 2, these values are more than enough to produce characteristic rotation spectra.

A possible inaccuracy arises in the above if the relative permittivity (ϵ_r) of the water within the wall is changed by the presence of the wall matrix. It is possible that the rotational mobility of this water is reduced so that water structured by the presence of biomacromolecules will have a relaxation frequency (f_c) between that of bulk water ($f_c \approx 20$ GHz) and that of ice ($f_c \approx 10$ kHz) [31]. The theoretical predictions of the extent of this change vary, but measurements (reviewed in Ref. 31) on water bound to proteins show relaxation frequencies between 100 MHz and 10 GHz: well above the region measured in the present work. This is confirmed by measurements on 'Sephadex' particles, which can be assumed to be a better model for the cell wall than proteins. The relaxation frequency of water within the Sephadex particles lies near 4 GHz [32]. It can therefore be assumed that cell-wall water will respond as bulk water to the field frequencies used here (2.5 MHz or less).

It is still possible that some property of the walls causes them to have an ϵ_r value different from that of bulk water. We modelled the effect on the rotation spectrum of a cell wall (0.3 μm thick and inner radius 3 μm) of varying the ϵ_r over the range of 30–160. A cell wall with $K_s = 5$ nS showed a variation of $\pm 12.5\%$ (with respect to the value at $\epsilon_r = 80$) in the amplitude of the rotation peak, which otherwise resembled curves e and f in Fig. 1. In the case of $K_s = 10$ nS, there was only $\pm 7.7\%$ variation in the amplitude of the rotation peak (again with respect to $\epsilon_r = 80$). The variation in ϵ_r also caused variations in the peak frequency: however, we only make use of the peak amplitudes in assigning a value to K_s (see following section). We conclude that even if ϵ_r is radically different from the value for water, the K_s value derived below is little affected.

Results and Discussion

(a) Rotation spectra

Hg(II)-treated cells showed a very different rotational spectrum from control cells (Figs. 3 and 4). In 10 μS/cm media, all affected cells had spectra which were indistinguishable from those seen after treatment with Ag^+ or with intense ultrasound [19]. Even those ultrasonically broken cells in which one end of the cell was completely broken away, or in which the wall had been split open along the long axis, showed rotation in this region. Therefore, the 0.8 MHz rotation was purely due to the wall material, and not due to a residual inner conductivity. However, the speed of rotation was rather slower than that shown in Fig. 3 (presumably for hydrodynamic reasons).

The absence of the anti-field rotation by treated

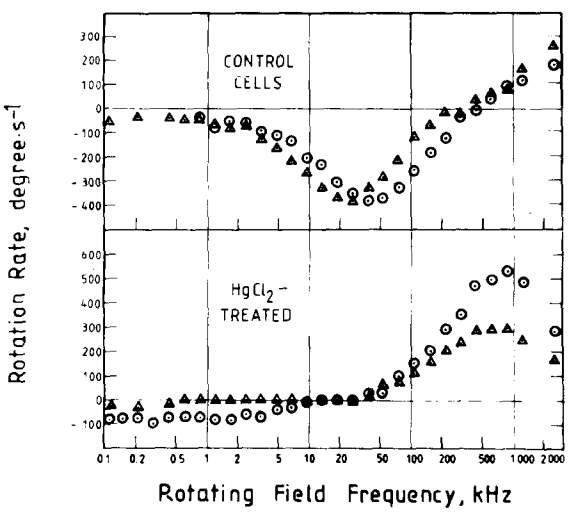

Fig. 3. Rotation spectra in media of 10 μS/cm conductivity of control yeast cells and of cells which had previously been incubated with $HgCl_2$ (18.4 μmol/l in 50 mM citric acid/KOH pH 4.5. 3 h). In each case, one plot is data from single cells (○), the other represents budded cells (△). Each plot is the mean of data from two cells of similar size and shape, which had been selected from many sets of data to be representative of their type. The field strength was the same as at 200 μS/cm (see legend to Fig. 2). Cell sizes: in each case the major and minor diameters are given in μm, the cells being treated as ellipsoids of rotation. Where two sets of dimensions are summed per cell, these describe the two components of a budded cell, measured as if they were two ellipsoids in contact. The control cells measured: (○) both cells 7.5·6.5; (△) 8.5·5.5 + 5.0·4.0 and 7.5·6.5 + 3.5·3.5. The $HgCl_2$-treated cells measured: (○) one cell 5.5·4.0, one cell 6.5·4.5; (△) both cells 6.5·4.0 + 5.5·4.0.

cells at 10 μS/cm indicates the the membrane conductivity had become very high (an extreme form of the trend shown by the theoretical curves 1c and 1d). It is not possible to conclude from this alone that the inside conductivity was affected, although it would be expected that extremely high membrane conductivities indicate a very 'leaky' membrane. In addition, analysis of the medium (section f below) indicated 100% K^+ leakage.

We have already explained that the co-field peak (at 0.8 MHz in 10 μS/cm media) exhibited by both damaged cells and cell walls can also be explained by the existence of a significant wall conductance. The spherical cell data in Fig. 3 show a ratio between co-field and anti-field amplitudes of 1.6 (= 550/350). The theoretical values for this ratio (curves 1c–f) at K_s values of 5 and 10 nS are 1.1 and 2.6, respectively. The value of the wall conductance can, therefore, be estimated to have been 7 nS. This value has been arrived at

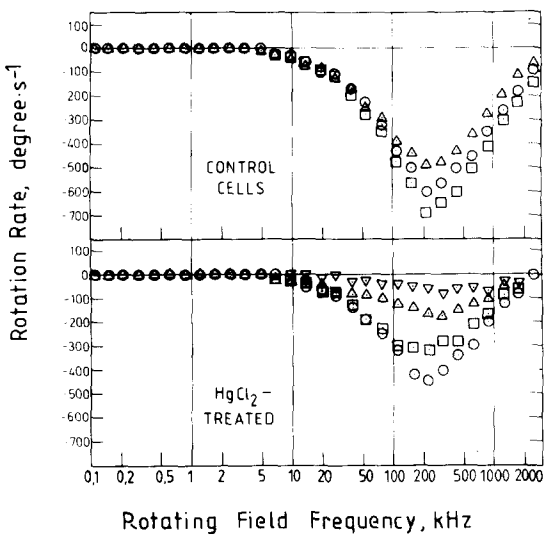

Fig. 4. Rotation spectra in media of 200 μS/cm conductivity of control yeast cells and of cells which had previously been incubated with $HgCl_2$ (3.7 μM in 50 mM citric acid/KOH pH 4.5, for 3 h). The rotating field was produced by applying a peak voltage difference of 15 volts between each pair of electrodes 1.4 mm apart. In most cases, the data points are from single measurements (not averages as in Fig. 3). Cell sizes: assuming cells and cell-buds to be ellipsoidal (see legend to Fig. 1), the major and minor axes measured (in μm) were as follows. Control cells; (△) mean of two cells 7.5·5.5 + 2.0·2.0 and 8.0·5.0 + 1.5; (○) 8.5·7.5; (□) 11.0·8.0. $HgCl_2$-treated cells: (▽) 7.0·5.0 + 6.5·5.0; (△) 8.0·6.5 + 5.5·5.0; (□) 8.5·6.0 + 5.5·5.0; (○) 9.0·6.5.

using data at a single conductivity and without having to consider the absolute rotation speeds. Substitution of this value into Eqn. 4 results in a value for the wall conductivity (at $\sigma_1 = 10$ μS/cm) of $\sigma_w = 33$ μS/cm.

It can be seen from Figs. 3 and 4 that the anti-field rotation of unaffected cells is slower in 10 μS/cm media than at 200 μS/cm, although this is not predicted by the theory for cells with no walls (curves 1a and 2a, respectively). Further, the frequency of the anti-field peak at 10 μS/cm is considerably higher than the theoretical curve (curve 1a), whereas the 200 μS/cm curve shows good agreement with the theory (curve 2a). This is also in accord with the possession by the cell wall of an appreciably higher conductivity than the medium. The cell membrane is thereby electrically screened, and this effect will be greater in 10 μS/cm medium than in 200 μS/cm media (where the ratio between wall and solution conductivities is lower, at least in bacteria [26,27]). The effect is illustrated by curves 1d and 1c.

We do not attempt to quantify the conductance using this sort of data because it is necessary to use the absolute rotation speed, or else to assume that the effect of the cell wall on rotation at 200 μS/cm is negligible. As can be seen by comparing Fig. 4 with curve 2b, at 200 μS/cm the cells rotated with only 50% of the theoretical speed. The discrepancy is not surprising in view of the fact that yeast cells are not perfect spheres, and do not possess the smooth surface that hydrodynamic theory demands. In addition, we can not rule out wall conductance effects. For both these reasons, quantitative analysis based on the absolute rotation speed is not advisable.

The models used for Figs. 1 and 2 predict that if the membrane resistivity had been completely abolished, there should have been no residual anti-field rotation at any conductivity. In 10 μS/cm media (Fig. 3), Hg(II)-treated cells either possessed no measurable anti-field rotation or were indistinguishable from control cells (the relative proportions depending on the amount of Hg(II) used). It seems that the membrane resistivity was abolished on an all-or-none basis. The all-or-none onset of membrane damage has often been reported in yeast cell populations affected by $HgCl_2$ [1,6] or other substances [33].

However, spectra taken in media of 200 μS/cm conductivity (Fig. 4) show that some treated cells exhibit intermediate strengths of anti-field rotation. The decreasing speeds of anti-field rotation in Fig. 4 correspond to decreasing membrane resistivities. Similar effects are shown either by cells that have the full internal conductivity (refer to the curve series 2a–d) or by cells in which the inner conductivity has been equilibrated with the medium (curves 2e–h). We do not attempt to quantitate the membrane conductivity because the cell wall conductance in 200 μS/cm media is unknown.

(b) Hg(II)-sensitivity and cell density

When the effect of a toxin on many cells must be measured, the taking of rotation spectra is too slow. We found it best to work at a fixed field frequency of 300 kHz, and to count the cells which rotated co-field in 10 μS/cm media. The results are expressed as the co-field rotation value defined above (Eqn. 1 in the Materials and Methods). Control incubations yielded few cells which rotate under these conditions (co-field rotation 10% or less). As the quantity of $HgCl_2$ or $Hg(NO_3)_2$ in the incubation was increased, the co-field rotation increased (Fig. 5). The sensitivity to Hg(II) was found to be higher after incubations using $1 \cdot 10^5$ cells/ml than when using $3 \cdot 10^6$ cells/ml (compare the extreme left and right hand curves of Fig. 5). The central curve shows a mean value for the sensitivity obtained from several experiments at $1 \cdot 10^5$ cells/ml.

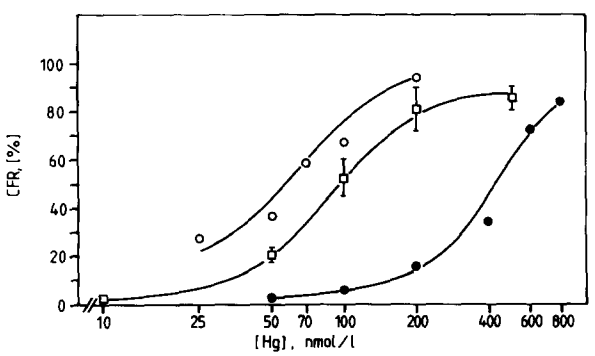

Fig. 5. The dose-response curves at two different cell concentrations for the $HgCl_2$-mediated change in rotation properties. The (□) symbols and error bars show the mean and deviation of at least 5 co-field rotation (CFR) values obtained on separate days (incubation density $1 \cdot 10^5$ cells/ml). Circular symbols refer to data obtained on a single day: (○) $1 \cdot 10^5$ cells/ml; (●) $3 \cdot 10^6$ cells/ml. The incubations were for 3 h and were unbuffered.

This effect of cell concentration on the co-field rotation value is better illustrated in Fig. 6. Although 400 nmol/l Hg(II) applied to $6 \cdot 10^4$ cells/ml gave 80% co-field rotation, there was little effect on $3 \cdot 10^6$ cells/ml. In the case of Ag^+ [19] it was argued that this cell-density effect is probably due to the binding of metal by the cell wall, which certainly occurs in the case of Hg(II) too [34,35]. However, quantitative interpretation is difficult because part of the Hg(II) binding is slow. For example, it has been observed that although the cell wall accounts for the greatest fraction of Hg(II) that is rapidly bound by yeast, longer incubations show some accumulation in the cell interior [34].

The cell concentration effect can help to explain why the co-field rotation method was much more sensitive (25–250 nmol/l) than other determinations of the toxicity of Hg(II) to yeast [6,21,36,37]. Table I shows that there is a clear inverse correlation between sensitivity and suspension density, despite the wide differences in media and incubation times.

It is interesting to note that no significant difference was found between the sensitivity to $HgCl_2$ or to $Hg(NO_3)_2$, despite the fact that $HgCl_2$ has a much greater stability constant [38]. This is because, at normal pH and in the absence of other ligands, low doses of any form of Hg(II) will be converted to $Hg(OH)_2$. For example, at pH 6.0

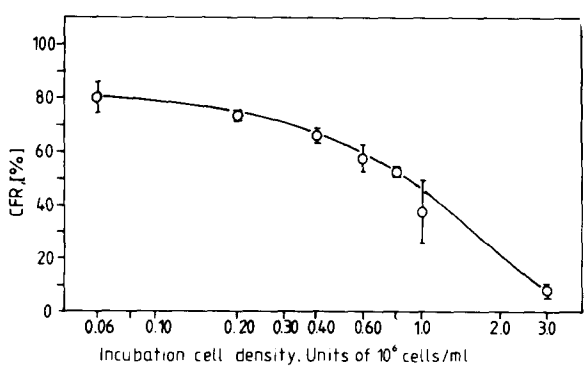

Fig. 6. The decrease in co-field rotation (CFR) obtained by increasing the cell density in the treatment medium (400 nmol/l $HgCl_2$ for 3 h in 12 mM Mes/KOH, pH 6.0).

TABLE I

COMPARISON OF THE SENSITIVITY OF *S. cerevisiae* TO Hg(II) REPORTED ELSEWHERE AND HERE

To enable comparison with the literature values, the cell densities that we used were re-calculated in mg/ml (the mean cell volume of the yeast used by us was 150 fl [19]). The results quoted are from Refs. (a) 6; (b) 36; (c) 21; (d) 37.

Criterion of toxicity	Toxic dose in assay (μmol/l)	Yeast concentration (initial) (mg/ml)	Assay medium	Source
50% K^+ release after 4 h	400	60	H_2O	[a]
50% inhibition of fermentation over 1–2 h	120	23	4% glucose	[b]
50% reduction in yield after 24 h growth	7.7	0.3	synth. growth medium	[c]
50% of cells showed no respiration after 30 min	0.8	8	0.85% NaCl	[d]
50% of cells	0.4	0.14	12 mM Mes/KOH	Fig. 4
showed co-field rotation	0.4	0.45	H_2O	Fig. 3
	0.1	0.015	H_2O	Fig. 3

the concentration of molecular $HgCl_2$ would first reach 10% of that of $Hg(OH)_2$ when the $HgCl_2$ dose was 18 μmol/l or more. However, these equilibrium-constant based calculations must be interpreted with caution because it has been reported that the majority of Hg(II) taken up by *Saccharomyces* [34] or by *Chlorella* [4] is irreversibly bound.

(c) Kinetics

The action of Hg(II) on yeast cells was found to be relatively slow (Fig. 7). In the case of amounts of Hg(II) near to the threshold, the co-field rotation was still increasing after 5 h of incubation,

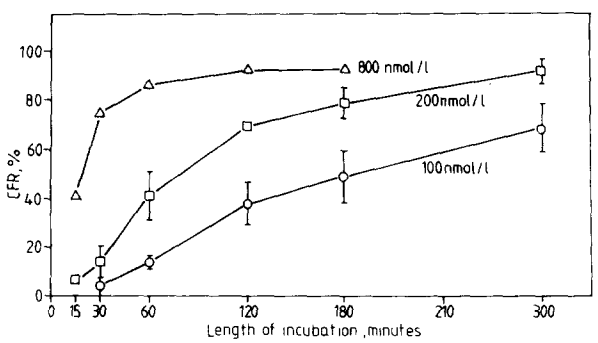

Fig. 7. Kinetics of the effect of $HgCl_2$ pre-treatment on yeast cell rotation. The curves for 100 nmol/l and 200 nmol/l show the means and deviations obtained from work on two days, whilst the 800 nmol/l curve refers to a single experiment. All incubations used $1 \cdot 10^5$ cells/ml and were unbuffered. CFR, co-field rotation.

and even 10 × threshold amounts required at least 1 h to reach saturation. A very fast (90 s) action of $HgCl_2$ (present at 1 mmol/l) on the respiration and permeability of yeast cells has been reported [39]. This is not necessarily at variance with the above because, in contrast to the $Hg(OH)_2$-dominated equilibria found in very dilute Hg(II) solutions, 1 mmol/l $HgCl_2$ will remain substantially in the molecular form. This is significant because $HgCl_2$ (but not $Hg(OH)_2$) is strongly membrane-permeant, at least in artificial bilayers [8,9]. Small amounts of $HgCl_3^-$ and $HgCl_4^{2-}$ will also be formed from 1 mmol/l $HgCl_2$ [7,10]. Therefore, other Hg(II)-transport mechanisms are to be expected in 1 mmol/l $HgCl_2$ from those seen at low concentrations.

(d) Effects of calcium and other salts

In contrast to the slow action of Hg(II) described above, Fig. 8 shows that addition of 1 mM $Ca(NO_3)_2$ after 20 or 60 min resulted in an immediate inhibition of the co-field rotation increase. This suggests that Ca^{2+} can compete for Hg(II) binding sites. It must also be said that the presence of Ca^{2+} will reduce the surface potential, leading to a local reduction in the concentration of all cations (including Hg^{2+}) near to the membrane [40]. Fig. 8 also shows that 1 mM calcium acetate gave a much stronger inhibition than did $Ca(NO_3)_2$: this was probably due to formation of mercuric acetate. This can be said because the presence of 2 mM acetate ion will have given a

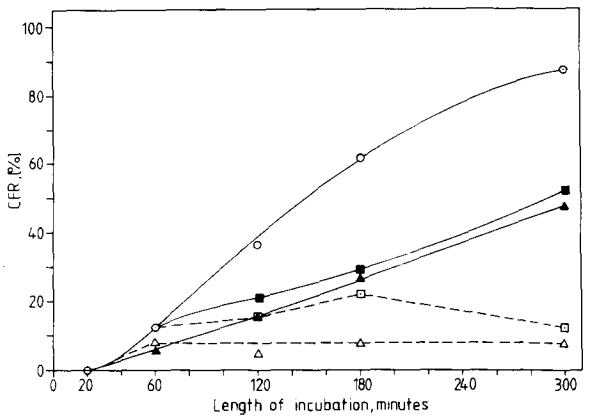

Fig. 8. Inhibition of the effect of $HgCl_2$ by the addition of 1 mM Ca^{2+} during the incubation. The data points represent: (○) controls, showing the progressive increase of co-field rotation (CFR) over 5 h; (■) $Ca(NO_3)_2$ added after 60 min; (▲) $Ca(NO_3)_2$ added after 20 min; (□) calcium acetate added after 60 min; (△) calcium acetate added after 20 min incubation. (2 μmol/l $HgCl_2$, $1 \cdot 10^5$ cells/ml in 50 mM citric acid/KOH, pH 4.5).

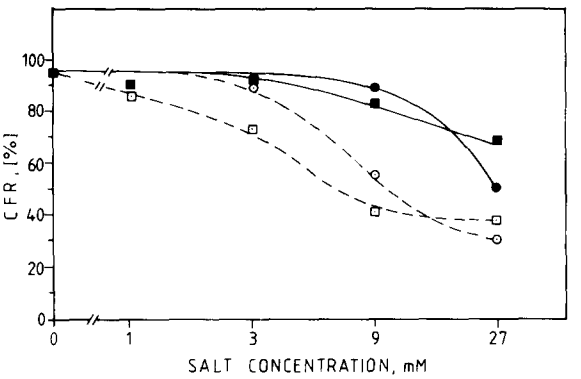

Fig. 9. Decrease in the effect of $HgCl_2$ on cell rotation in response to the presence of increasing concentrations of KNO_3 (circular symbols) or $NaNO_3$ (square symbols) in the incubation medium. The $HgCl_2$ concentrations were: (●, ■) 400 nmol/l; (○, □) 200 nmol/l.

mercuric acetate/Hg^{2+} concentration ratio of $4 \cdot 10^4$, whereas the ratio between $Hg(OH)_2$ (otherwise the dominant species) and Hg^{2+} at pH 4.5 is 630. Therefore, the formation of mercuric acetate will have reduced the concentration of all other Hg(II) species by a factor of $4 \cdot 10^4/630 = 63$. The values are calculated from data from the tables of Ref. 38.

It is also possible that the effects of acetate are due to diffusion of acetic acid across the membrane leading to a reduction in cytoplasmic pH, and so to a change in sensitivity to Hg(II) at a cytoplasmic site. We tested the effects of acetate alone by carrying out similar experiments to those shown in Fig. 8, but using 2 mM potassium acetate in parallel to 1 mM calcium acetate. Although potassium acetate alone did protect against the effects of Hg(II), the calcium salt gave at least double the effect (although the acetate concentration was the same).

The above observations (of slowly developing damage to the cells which can be rapidly inhibited) suggests a two-stage model for the action of Hg(II). The initial binding is fast and reversible, and is the obligatory precursor of a slower, irreversible, permeabilising reaction. The observation that the increase in co-field rotation is extremely slow at 20 °C may mean that the irreversible stage is highly temperature dependent. A fast (ionic ?) binding followed by transport-limited or other slow but damaging processes have often been proposed for the mechanism of damage by Hg(II) [4,6,9,10].

Fig. 9 shows that 3–30 mM KNO_3 or $NaNO_3$ are also capable of decreasing the action of Hg(II). The fact that K^+ salts were not found to have a stronger effect than their Na^+ analogues indicates that neither the membrane potential nor K^+-specific sites are involved (in contrast to the Ag^+ sensitivity found earlier [19]).

(e) pH dependence

It was observed that the sensitivity to Hg(II) decreased as the pH was increased. The central curve of Fig. 10 shows the effect well, although it is possible that these values were affected by the salt-concentration effect (Fig. 9), because increasing pH values were accompanied by progressive increases in K^+ concentration. However, even when the K^+ concentration was held constant (upper and lower curves of Fig. 10), the effect of pH change is still to be seen. It is known that the surface charge of yeast cells and cell walls becomes more negative as the pH increases [41,42]. This may give a greater binding of Hg^{2+}, as was measured in the case of Mn^{2+} [35]. This will amplify the suspension-density effect (Fig. 6) at high pH.

It can be argued that the rapid decrease in the

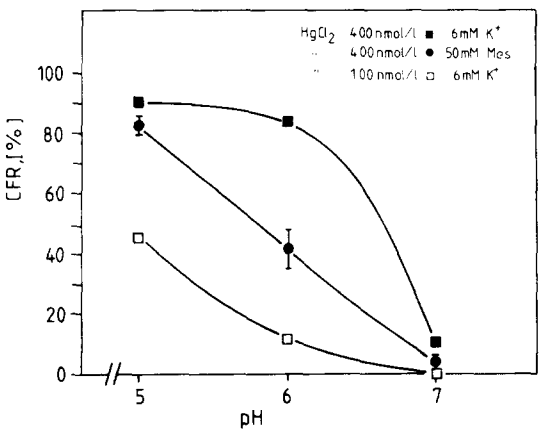

Fig. 10. Decrease in $HgCl_2$ sensitivity with increase of pH. The experimental difference between the circular and square symbols was that either the K^+, or the Mes concentration was held constant over the pH range. The incubation conditions were: (■) 400 nmol/l $HgCl_2$ in 6 mM KOH/Mes; (●) 400 nmol/l $HgCl_2$ in 50 mM Mes/KOH; (□) 100 nmol/l $HgCl_2$ in 6 mM KOH/Mes.

concentration of Hg^{2+} with increasing pH (due to $Hg(OH)_2$ formation, as noted in connection with Fig. 5) could contribute to the pH sensitivity. This is because a pH increase from 4.5 to 6.0 should decrease the concentration of free Hg^{2+} (already extremely low) by a factor of 1000. However, Fig. 10 shows that to maintain 50% co-field rotation

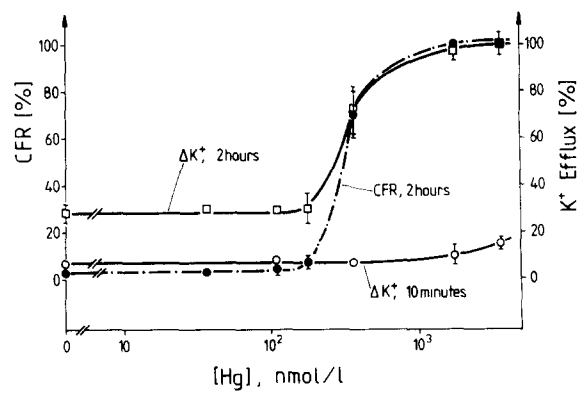

Fig. 11. Comparison between the percentages of potassium lost by the cells (open symbols) and the change in the rotation parameter co-field rotation (solid circles) that resulted from the addition of various amounts of $HgCl_2$. The two steeper curves refer to cells that had been incubated for 2 h, whilst the flatter curve shows the very small K^+ efflux that could be measured after 10 min incubation.

over this pH range it is only necessary to increase the $HgCl_2$ dose by a factor of 4. Therefore, the change in free Hg^{2+} concentration cannot explain the pH dependence.

(f) K^+ release

The action of Hg(II) on yeast cells is known to cause the release of most of the K^+ [6]. This was also found to be the case here, and the increase in co-field rotation correlated very well with this release (Fig. 11). In both cases little effect was seen after only 10 min of incubation, but after 2 h, 100% of the K^+ loss and 100% co-field rotation were reached. It should be noted that even in control incubations, about 30% of the cellular K^+ is lost after 2 h (as is normal in a K^+-free medium [1]). Despite this there was no change in the co-field rotation, which means that the 30% K^+ loss was evenly distributed over the cells. If 30% of the cells had lost essentially all their K^+, even without incurring a drastic decrease in membrane resistivity, these cells would have given rise to a corresponding co-field rotation value.

Conclusion

We have demonstrated that the single-cell rotation technique can be modified to follow the effects of Hg(II) on yeast cells. The quantities of Hg(II) that can be detected in this way appear to be smaller than possible with other bio-assays, which is largely a consequence of the ability to work with very small numbers of cells. A further advantage of the single-cell rotation technique is that we were able to observe directly deviations from the all-or-none response.

As part of the investigation of the Hg(II)-treated yeast cells it was noted that their rotation in response to rotating fields between 0.1 and 2500 kHz was indistinguishable from that of yeast cell walls. This rotation could only be accounted for by assuming that the yeast wall has a conductivity (33 μS/cm), which is rather higher than that of our assay medium (10 μS/cm). Literature values for the cell wall conductivities of many bacteria are considerably higher (3–9 mS/cm) than this, so the rotation method may find application in the characterisation of microbial wall composition and structure. It may also be possible to follow the

binding of substances to ionogenic groups within the wall.

Acknowledgements

The apparatus used was built and maintained with the expert technical help of Mr. W. Virsik, Mr. U. Remmel, Mr. A. Gessner and Mr. W. Hupp. This work was supported by a grant (No. 10603035/2) from The Umweltbundesamt, Berlin to U.Z.

References

1 Rothstein, A. and Bruce, M. (1958) J. Cell. Comp. Physiol. 51, 439–455
2 Sugiura, Y. and Koga, S. (1965) Biophys. J. 5, 439–445
3 Vallee, B.L. and Ulmer, D.D. (1972) Ann. Rev. Biochem. 41, 91–128
4 Barber, J., Beauford, W. and Shieh, Y.J. (1973) in Mercury, Mercurials and Mercaptans (Miller, M.W., Clarkson, T.W., eds.), pp. 325–345, Charles C. Thomas, Springfield, Illinois
5 Schweiger, G., Sellner, M., Golle, B. and Lüttge, U. (1983) Ecotoxicology and Environmental Safety 7, 366–372
6 Passow, H. and Rothstein, A. (1960) J. Gen. Physiol. 43, 621–633
7 Hahne, H.C.H. and Kroontje, W. (1973) Soil. Sci. Soc. Am. Proc. 37, 838–843
8 Gutknecht, J. (1981) J. Membrane Biol. 61, 61–66
9 Bienvenue, E., Boudou, A., Desmazes, J.P., Gavach, J., Georgescauld, D., Sandeaux, R. and Seta, P. (1984) Chem. -Biol. Interactions 48, 91–101
10 Boudou, A., Georgescauld, D. and Desmazes, J.P. (1983) in Aquatic Toxicology (Nriagu, J.O., ed.), pp. 117–136, John Wiley and Sons, Inc., New York
11 Zimmermann, U. and Arnold, W.M. (1983) Coherent Excitations in Biological Systems (Fröhlich, H. Kremer, F., eds.), pp. 211–221, Springer-Verlag, Berlin
12 Glaser, R., Fuhr, G. and Gimsa, J. (1983) Studia Biophysica 96, 11–20
13 Arnold, W.M., Wendt, B., Zimmermann, U. and Korenstein, R. (1985) Biochim. Biophys. Acta 813, 117–131
14 Schwan, H.P. (1985) Studia Biophysica 110, 13–18
15 Sauer, F.A. and Schlögl, R.W. (1985) in Interactions Between Electromagnetic Fields and Cells (Chiabrera, A. Nicolini, C. Schwan, H.P., eds.), pp. 203–251, Plenum Press, New York
16 Fuhr, G.R. (1985) Dissertation, Humboldt-Universität, Berlin
17 Fuhr, G.R., Glaser, R. and Hagedorn, R. (1986) Biophys. J. 49, 395–402
18 Asami, K. (1977) Bull. Inst. Chem. Res. 55, 283–309
19 Arnold, W.M., Geier, B.M., Wendt, B. and Zimmermann, U. (1986) Biochim. Biophys. Acta 889, 35–48
20 Arnold, W.M. and Zimmermann, U. (1984) in Biological Membranes, Vol. 5 (Chapman, D., ed.), pp. 381–444, Academic Press, London
21 White, J. and Munns, D.J. (1951) J. Inst. Brew. 57, 175–179
22 Ramamorthy, S. and Kushner, D.J. (1975) Microb. Ecology 2, 162–176
23 Gadd, G.M. and Griffiths, A.J. (1978) Microbial Ecol. 4, 303–317
24 Agar, H.D. and Douglas, H.C. (1955) J. Bacteriol. 70, 427–434
25 Arnold, W.N. (1981) in Yeast Cell Envelopes: Biochemistry, Biophysics, and Ultrastructure (Arnold, W.N., ed.), Vol. 1, pp. 25–47, CRC Press Inc. Boca Raton, FL
26 Carstensen, E.L., Cox, H.A., Mercer, W.B. and Natale, L.A. (1965) Biophys. J. 5, 289–300
27 Carstensen, E.L. and Marquis, R.E. (1968) Biophys. J. 8, 536–548
28 Arnold, W.N. and Lacy, J.S. (1977) J. Bacteriol. 131, 564–571
29 Scherrer, R., Louden, L. and Gerhardt, P. (1974) J. Bacteriol. 118, 534–540
30 Neihof, R. and Echols, W.H. (1973) Biochim. Biophys. Acta 318, 23–32
31 Pethig, R. (1979) Dielectric and Electronic Properties of Biological Materials. John Wiley and Sons, Chichester
32 Koide, G.T. and Carstensen, E.L. (1976) J. Phys. Chem. 80, 55–59
33 Borst-Pauwels, G.W.F.H. and Theuvenet, A.P.R. (1985) FEMS Microbiol. Lett. 29, 221–224
34 Murray, A.D. and Kidby, D.K. (1975) J. Gen. Microbiol. 86, 66–74
35 Rothstein, A. and Hayes, A.D. (1956) Arch. Biochem. Biophys. 63, 87–99
36 Baas Becking, L.G.M., Van Iterson, G., Kloos, A.W., Koningsberger, V.J., Pulle, A.A., Schoute, J.C., Stomps, T.J., Verdoorn, F., Weevers, T. and Zijlstra, K. (1940) Recueil des Travaux Botaniques Néerlandais 37, 43–77
37 Bitton, G.B., Koopman, B. and Wang, H.-D. (1984) Bull. Environ. Contam. Toxicol. 32, 80–84
38 Smith, R.M. and Martell, A.E. (1976) Critical Stability Constants, Vol. 4, Plenum Press, New York
39 Brunker, R.L. (1976) Appl. Environ. Microbiol. 32, 498–504
40 Gage, R.A., Van Wijngaarden, W., Theuvenet, A.P.R. Borst-Pauwels, G.W.F.H. and Verkleij, A.J. (1985) Biochim. Biophys. Acta 812, 1–8
41 Eddy, A.A. and Rudin, A.D. (1958) Proc. Roy. Soc. B. 148B, 419–432
42 Fuhrmann, G.F., Boehm, C. and Theuvenet, A.P.R. (1976) Biochim. Biophys. Acta 433, 583–596